

System Engineering Study of Electrodynamic Tether
as a Spaceborne Generator and Radiator of Electromagnetic Waves
in the ULF/ELF Frequency Band

NASA Grant NAG8-551

Semiannual Report #1

For the period 1 September 1985 through 28 February 1986

Principal Investigator

Dr. Robert D. Estes

March 1986



Prepared for
National Aeronautics and Space Administration
Marshall Space Flight Center, Alabama 35812

Smithsonian Institution
Astrophysical Observatory
Cambridge, Massachusetts 02138

The Smithsonian Astrophysical Observatory
is a member of the
Harvard-Smithsonian Center for Astrophysics

The NASA Technical Officer for this Grant is
Dr. Georg F. von Tiesenhausen, Code PS01, Advanced
Systems Office, Marshall Space Flight Center, Alabama 35812

(NASA-CR-176749) SYSTEM ENGINEERING STUDY
OF ELECTRODYNAMIC TETHER AS A SPACEBORNE
GENERATOR AND RADIATOR OF ELECTROMAGNETIC
WAVES IN THE ULF/ELF FREQUENCY BAND
Semiannual (Smithsonian Astrophysical
G3/32 42914
Unclas
N86-25689

System Engineering Study of Electrodynamic Tether as a
Spaceborne Generator and Radiator of Electromagnetic Waves
in the ULF/ELF Frequency Band

NASA Grant NAG8-551

Semiannual Report #1

For the period 1 September 1985 through 28 February 1986

Principal Investigator

Dr. Robert D. Estes

Co-Investigators

Dr. Mario D. Grossi
Dr. Enrico C. Lorenzini

March 1986

Prepared for

National Aeronautics and Space Administration
Marshall Space Flight Center, Alabama 35812

Smithsonian Institution
Astrophysical Observatory
Cambridge, Massachusetts 02138

The Smithsonian Astrophysical Observatory
is a member of the
Harvard-Smithsonian Center for Astrophysics

CONTENTS

		Page
SECTION 1.0	INTRODUCTION	3
2.0	THE BASICS OF POWER CONSUMPTION BY "SELF-DRIVEN" RADIATING TETHER SYSTEMS	6
3.0	REDUCING POWER CONSUMPTION BY RADIATING TETHER SYSTEMS . .	15
4.0	TETHER RADIATION AND THE QUESTION OF TETHER LENGTH	22
5.0	SYSTEM CONFIGURATION: ONE TETHER VS. TWO	32
6.0	DYNAMICS OF THE DUAL TETHER ULF/ELF SYSTEM	34
7.0	CONCLUSIONS AND FUTURE WORK	44
8.0	REFERENCES	46

1.0 INTRODUCTION

There are two basic questions to be answered. First, can orbiting tethered satellite systems generate and transmit information-carrying electromagnetic waves in the ULF/ELF frequency band to the earth at suitably high signal intensities? Second, can such systems be maintained in their orbits for suitably long periods of time without excessive on-board power requirements? These questions are not really independent of each other, because the current values required to generate sufficiently strong signals determine how much on-board power is required to counteract orbital decay due to electrodynamic drag and to run the system in its reversed current phase.

The problem of ULF/ELF wave generation and propagation from a tethered system to the earth is extremely complicated. It cannot be said by any means to have been solved. Nonetheless, sufficient progress has been made to enable us to make some estimate of how much power will be injected into electromagnetic waves as a function of system parameters such as tether length and orbital height. Based on these estimates we have some idea of the range of radiation resistances that might be reasonably attained. Then, leaving aside the unsolved problem of ionospheric crossing losses, we can make estimates of on-board power requirements for orbiting ULF/ELF tether systems assuming different levels of radiated power. These estimates then allow us to see if the required on-board power levels are attainable by systems of reasonable size and complexity. This has been the main thrust of the first six months of our investigation.

The study began with a candidate system, one that we refer to as the "self-driven" system, because it stores part of the electrical energy generated by the tether motion in the natural current phase and then utilizes that energy to help

drive the current in the reversed, electrodynamic thrust, phase of operation.

Section 2 presents the basic equations needed to evaluate alternating current tethered systems from the standpoint of external energy (on-board, or external to the tether-ionosphere system) requirement. They are quite simple. All the complexity lies in the calculation of the radiation resistance and the determination of necessary radiated power levels.

In Section 3, we apply the basic energy equations to tethered systems with various lengths, tether resistances, and radiation resistances, operating at different current values. This is done for systems with and without the "self-driven" mechanism.

The result that emerges from these calculations is that shorter tethers are definitely preferred from the standpoint of minimizing on-board power requirements. If it were possible to maintain a sufficiently high radiation resistance for short tether lengths (5-10 km, say), then it might be possible to forego the use of the "self-driven" mechanism. The question of radiation resistance as a function of tether length and orbital height is discussed in Section 4. Should fairly long (20-50 km) tethers prove to be necessary, the "self-driven" concept, combined with the use of low resistance tethers, is capable of reducing the power requirements very substantially - at the expense of radiated power, which may be limited by the amount of current the ionosphere can carry, in any case. Tables I through IV at the end of Section 3 summarize the results. The external power requirements for these examples are seen to be only a few kilowatts, or even less than a kilowatt, in a number of cases. Again, we point out that radiated power requirements have yet to be determined. For what we believe to be reasonable estimates of system parameters, however, ULF/ELF continuously radiating systems could be maintained in orbit with moderate power requirements.

Section 4 considers in some detail the effect of tether length on the power going into electromagnetic waves. We conclude that waves from the tether belong to two separate classes. There are the transmission line waves which carry current down the geomagnetic field lines. These are identical with the Alfvén waves. Then there are waves emitted by the tether functioning as a long electric dipole type antenna, as the current is reversed back and forth through the tether. The wave impedance, or radiation resistance, variation with tether length is markedly different for the two classes of waves. Thus, determining which is preferable from the standpoints of propagation through the ionosphere and signal carrying ability is important. The answer to this question will have a significant impact on system design and operating parameters. Initial estimates are given for radiation resistances as a function of tether length, orbital height, and day/night variation for the two classes of waves.

In Section 5 we discuss the question whether a single or dual tether system is preferable for the self-driven mode of operation. The tentative conclusion is that the single tether system is preferable. The dynamics of the two tether system are examined in Section 6.

We summarize our conclusions from the first part of the investigation and outline our continuing efforts in Section 7. Special attention will be given to signal encoding methods in the upcoming months as well as to the assessment of energy storage and primary power sources.

2.0 THE BASICS OF POWER CONSUMPTION BY "SELF-DRIVEN" RADIATING TETHER SYSTEMS

We approach the problem from the energetic standpoint, which gives us results that are independent of the specific type of energy storage or power transfer system that is used.

We first consider the tethered system in its "natural" current drawing mode, i.e. in the phase for which current flows strictly due to the emf induced by the system's orbital motion across the terrestrial magnetic field. This is illustrated in Figure 2.1, where we assume an eastward motion and upward deployment. For simplicity of illustration, we show the case for which the tether (connecting satellite S and S_1), the magnetic field \vec{B} , and the orbital velocity \vec{v} are mutually perpendicular. The results we obtain are completely general, however. A current i flows up the tether (electrons flowing down the tether). Current also flows through the ionosphere along magnetic field lines. We show this current as being evenly divided between the two directions along the field lines in Figure 2.1.

In the tether rest frame, the equivalent circuit is conveniently represented by Figure 2.2(a). The motion induced emf is shown as $V_B = vBl$, where l is the tether length. R_t is the tether resistance, R_{ion} is the radiation resistance of the ionosphere, and Z_L is the load impedance of the system being used for energy storage on satellite S. We assume the contact resistances between the satellite S_1 and the ionosphere and between satellite S and the ionosphere are kept at negligible levels by the use of plasma contactors. This simplifying assumption is not essential. The D-C resistance R_t of the tether can be considered constant. For current levels below some critical value, at least, the radiation resistance should also be nearly constant over a time in-

terval short enough to maintain nearly constant values of plasma density and temperature. We assume that the time period T during which we draw the current in the "natural" mode satisfies this criterion.

In this case, the current i flowing in the tether-ionosphere current loop varies depending on the value of Z_L , the load impedance, since

$$i = \frac{V_B}{R_t + R_{ion} + Z_L} \quad (1)$$

This is the current that would flow due to a voltage

$$V' = V_B - i Z_L \quad (2)$$

if only the tether and ionosphere were considered, as shown in Figure 2.2(b). This, then, is the voltage we have to obtain in the reverse sense if we want to have the current reversed, but with the same absolute value, in the second phase of operation.

We desire this in order to gain an electrodynamic thrust that makes up for the drag experienced in the "natural" current phase of operation and to radiate electromagnetic waves from the tether functioning as an antenna.

The power into the load is $i^2 Z_L$. Assuming for the moment 100% efficiency, the total energy that is stored in the natural current phase is given by:

$$E_{STORED} = i^2 Z_L T \quad (3)$$

where T is the period of the natural current phase.

This energy is available for a contribution to the reversed current mode operation.

Figure 2.3 illustrates the equivalent circuit for the reversed current mode. The motion induced emf V_B is still part of the circuit. There is now an applied voltage V_R which acts in the direction opposite to V_B and which drives the current in the opposite direction. We assume that this current is being driven through the same tether as in Figure 2.1 or that, if the current is driven through a tether connecting satellite S to a lower satellite S_2 (as in Figure 2.4), the second tether is identical to the first.

From equation (2) we see that the voltage V_R necessary to drive the current i in the reversed sense is given by:

$$V_R = V' + V_B = 2V_B - iZ_L \quad (4)$$

To sustain this reversed current for a period of time T equal to that of the natural current phase requires an energy $E_R = i V_R T$.

Combining equations (1) and (4) gives:

$$E_R = \left[2 i^2 (R_t + R_{ion}) + i^2 Z_L \right] T \quad (5)$$

The last term in this expression is $i^2 Z_L T$, which is just the energy stored of equation (3).

Thus the energy that must be supplied from an external power service, i.e. by solar cells or batteries is seen to be:

$$E_{\text{ext}} = 2i^2 (R_t + R_{\text{ion}})T \quad (6)$$

the amount of energy dissipated in the two phases of operation.

The average external power required is given by:

$$\bar{P}_{\text{ext}} = i^2 (R_t + R_{\text{ion}}) \quad (7)$$

This result -- its functional dependence on i , R_t , and R_{ion} , that is -- is independent of Z_L . It depends on V_b and Z_L through equation (1). The average external power required in expression (7) represents the thermodynamic minimum. Dissipated energy represents an unrecoverable loss. There would be an additional amount of external power required to make up for conversion losses, which we have taken to be zero. We will consider this effect later.

We have driven the current in the reversed sense for a time T equal to the time of "natural" current flow. Thus, always assuming constant \vec{B} and $\delta v \ll v$, where δv is the change in orbital velocity due to the electrodynamic drag, we have made up in the second (reversed current) part of our cycle for the orbital energy lost in the first part.

We will be examining the effects of relaxing these assumptions in the next six months of our investigation. For now, it seems both reasonable and expedient to ignore them, since we want to get to the more important questions of feasibility.

Having derived the simple basic equations (1) and (7), we are now in a position to examine their consequences for a partially self-powered radiating tethered satellite system.

It is immediately apparent from equation (7) that, whatever the current value, the required external power will be reduced if the tether resistance R_t is reduced. We can maintain a given current level while reducing R_t (maintaining the same tether length ℓ) by increasing Z_L , and hence increasing the energy stored in the first part of the cycle. This is seen from equation (1).

Thus there is a premium on using tethers with low resistance values per unit length. For now we are assuming that tether length is not one of the parameters we can vary. We assume it to be fixed by the desired radiation resistance and the wavelength of our radiation.

We also assume that there is a certain current level below which we do not want to go because of the radiated power levels we require. By making some estimates of what tether lengths and current values might be used in an actual system we are able to clearly demonstrate the feasibility and advantages of maintaining radiating tethered systems in orbit for long periods of time by the use of the "self-driven" reverse current thrust mode of operation. A number of cases are summarized in the tables of the following section. The required average external power is well within the reach of solar cells of reasonable size for a number of the parameter combinations. This claim will be made more concrete in the next six months.

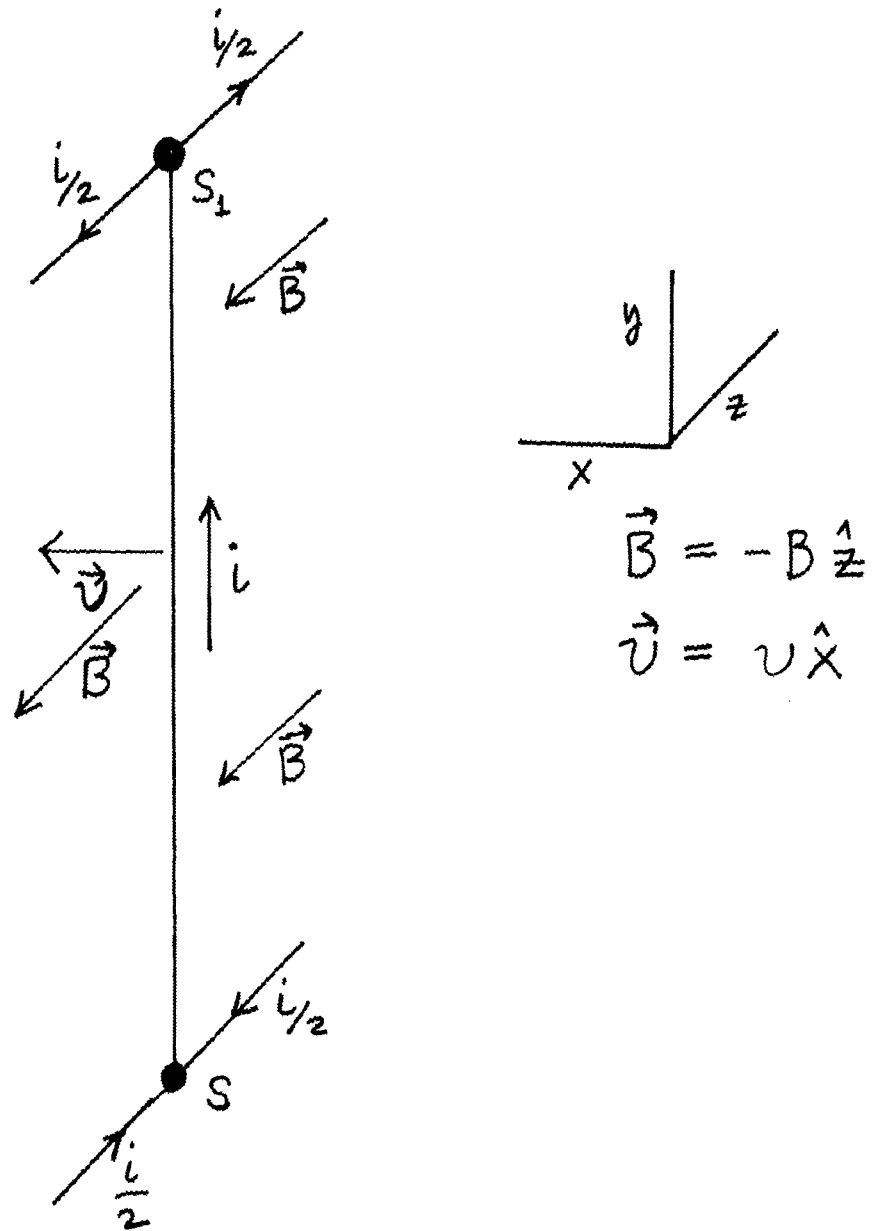


Figure 2.1

System Configuration and Currents

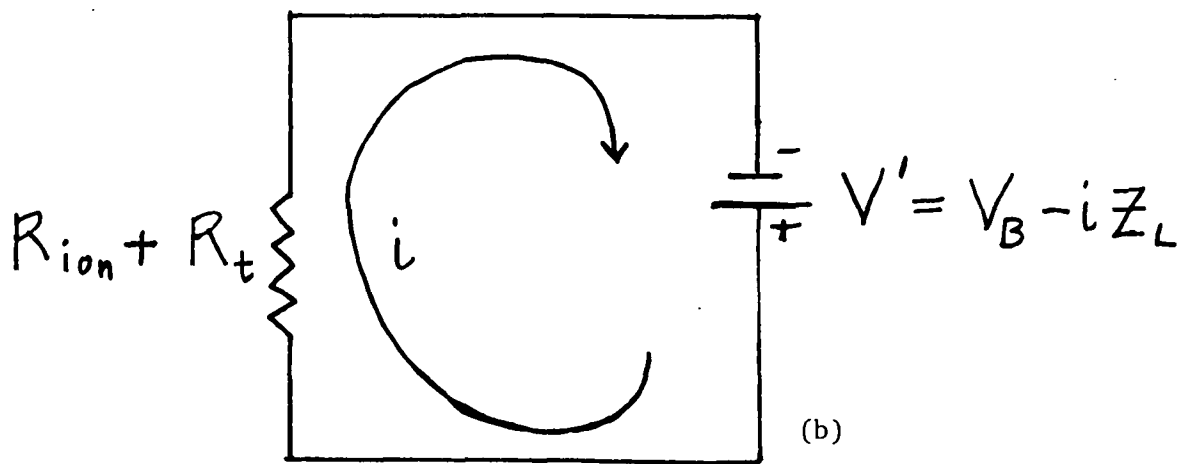
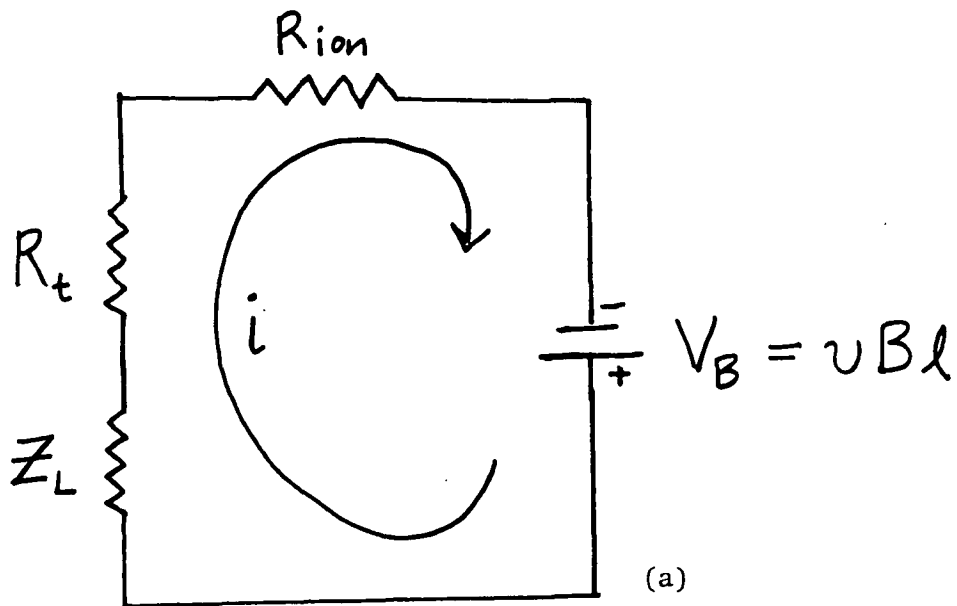


Figure 2.2

Equivalent Circuits for Tether/Ionospheric "Natural" Current Mode.

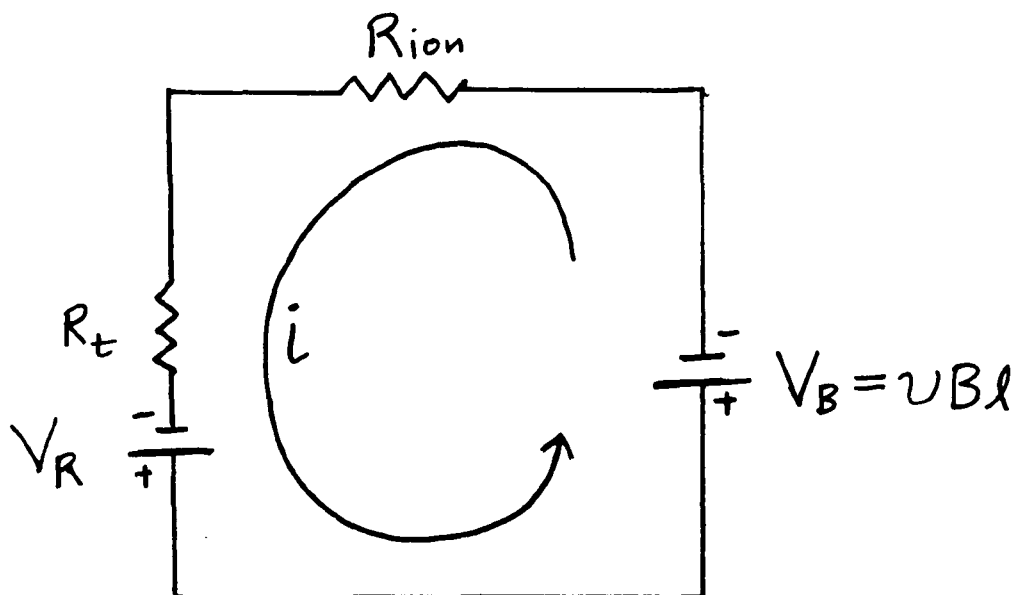


Figure 2.3

Equivalent Circuit for Tether Reversed Current Mode

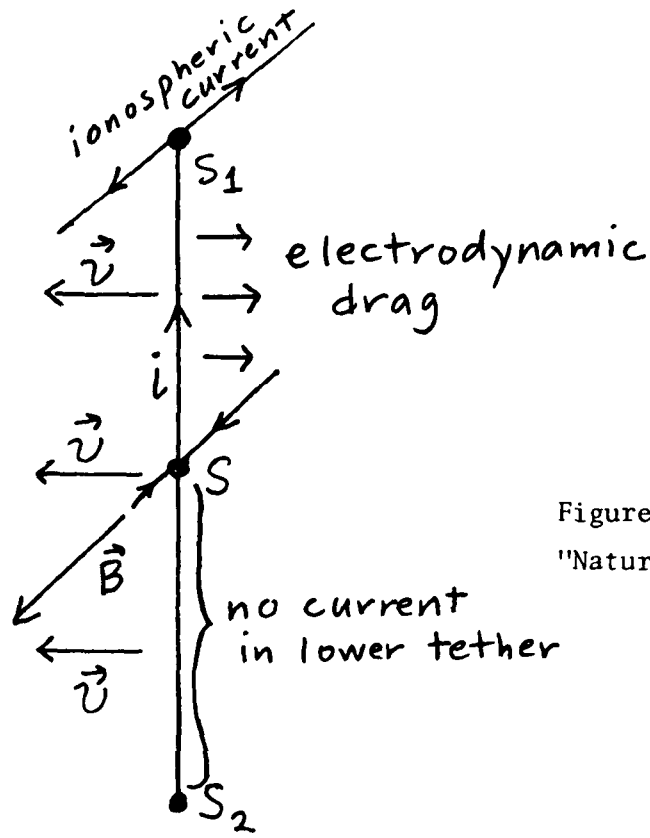


Figure 2.4 (a)
"Natural" Current Phase

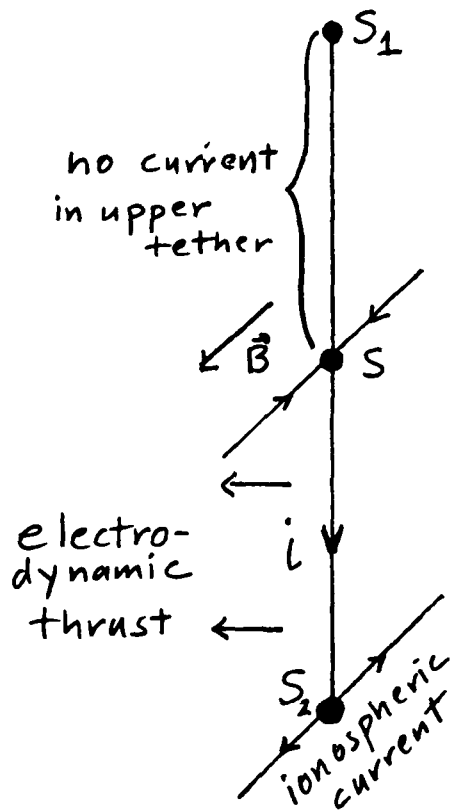


Figure 2.4 (b)
"Reversed" Current Phase

Figure 2.4. The Dual Tether System

3.0 REDUCING POWER CONSUMPTION BY RADIATING TETHER SYSTEMS

Tables I through IV display for a number of system parameter combinations the on-board power requirements to operate an electrodynamic tethered system radiator. This important quantity - the on-board power required - is given in the bottom row of each table as \bar{P}_{ext} the average external power, calculated from equation (7).

We want to make it clear that the values chosen for R_{ion} , the radiation resistance, are not based on experimental evidence or reliable calculations. Since this quantity is of fundamental importance in the problem of e.m. radiation and not yet well known, we have considered cases of $R_{\text{ion}} = 2\Omega$, 10Ω , and 50Ω . R_{ion} may in fact vary considerably with the frequency of tether current oscillation. Barnett and Olbert (1986) obtained values ranging from less than 1Ω (ULF) to tens of thousands of ohms (for frequencies greater than the lower hybrid frequency $f_{\text{LH}} \approx 7\text{kHz}$ at 300 km). Unfortunately, we have not thus far received funding for a parallel study that we had hoped to make, which would have included calculations of the radiation resistance, as well as of ionospheric crossing losses. The values of radiation resistance we have chosen do lie, we believe, within a range that is reasonable to consider for purposes of illustration and comparison. At the upper end (50Ω) the radiation resistance becomes comparable to or larger than the resistance of the tether in some of the cases considered.

Tables I and II are for tether lengths of 20 km and 5 km, respectively, in the case where none of the motion-generated power of the natural current phase of operation is utilized to drive the reverse current of the second phase.

Tables III and IV may be compared column by column with Tables I and II for columns (a) - (e) to show the effect of reducing tether resistance (per unit length) and at the same time maintaining constant current and radiated power values by utilizing some of the motion-induced electrical power (an amount $i^2 Z_L$) to provide a portion of the power necessary to run the system in the reversed current mode of operation.

Furthermore, the two additional columns (f) and (g) of Tables III and IV demonstrate the effect of this kind of power utilization for cases where the tether resistance is maintained at a fixed value and the current and power radiated values necessarily drop. This would correspond to the case where the "self-driven" thrust capabilities were utilized only part of the time. A comparison of columns (f) and (g) of Tables III and IV with columns (b) and (a) of Tables I and II demonstrates a general fact: for constant R_t and R_{ion} , the ratio of the radiated power to the average external power required P_{rad}/\bar{P}_{ext} is a constant, independent of Z_L . This will be discussed more fully below.

To illustrate how the tables may be used, we begin by considering each column of Table I. Table I corresponds to a system for which none of the motion-induced electrical power is stored. All of the power required to run the system in the reversed current mode must be supplied by a satellite-borne power source. The different columns of the table correspond to different values of the radiation resistance R_{ion} and the power radiated P_{rad} . The tether resistance values R_t are chosen to correspond to the current values necessary to maintain the given P_{rad} level. Since neither the P_{rad} requirements nor the actual R_{ion} values that will obtain are known, we have chosen several different combinations. Lowering R_t would of course increase the current i and hence the power radiated P_{rad} . A comparison of columns (b) and (c) and of columns (d) and (e) illustrates this. We have not allowed current values above 11.2 A since

there probably exists an upper limit to the current that can be drawn through the ionosphere. The external power requirements are seen to be high (17.5 kW - 39.1 kW) for all the cases considered. Lowering the tether resistance R_t , by itself, only makes matters worse from the energy requirement standpoint. The power radiated increases as R_t decreases, but so does \bar{P}_{ext} . This is also illustrated by a comparison of columns (b) and (c) and of (d) and (e).

Table II repeats the calculations of Table I, only for a system with tether length 5 km. All of the comments made above concerning comparisons between different columns of Table I apply to Table II as well. It should be kept in mind, however, that radiation resistance for a given frequency could be strongly dependent on tether length. Thus column (b) of Table II, for example, might be a more reasonable comparison to column (a) of Table I than column (a) of Table II is.

One point, however, is clear from a comparison of Tables I and II. Everything else being equal, a shorter tether length requires less external power. This is due to the lower motion-induced voltage V_B , which depends directly on the tether length. For a fixed current value, a lower R_t corresponds to this lower V_B ; and a lower V_B value means that less power is required to overcome V_B in the reversed current mode. Table II is entirely for cases with no energy storage in the natural current phase. The average external power requirements range from 4.4 kW to 9.8 kW, a decided improvement over the cases considered in Table I, but still undesirably high.

Table III relates mainly to 20 km tether systems with low resistance ($R_t/\ell=5\Omega/\text{km}$) for which the self-driven thrust concept has been utilized. These cases are shown in columns (a)-(e). The values of R_{ion} , i , V_B and P_{rad} for each of these columns are identical to those in the corresponding column in Table I.

The differences are only in the R_t , Z_L , $i^2 Z_L$, and hence \bar{P}_{ext} values. The cases that required 17.5 kW of external power in the (Table I) systems with high tether resistance and no utilization of the self-driven thrust mechanism required only 2.55 to 3.75 kW of external power when low resistance tethers are used with the self-driven thrust system. The 11.2A cases that required 39.1 kW in the system with no utilization of the natural current mode power had external power requirements reduced to 12.75-13.75 kW, which are still high but are reduced by around 2/3 from the Table I value. This is accomplished with no reduction in radiated power.

Table III, in its last two columns, demonstrates the effect of using the self-driven concept without reducing the tether resistance. The external power requirements become smaller because the introduction of the load impedance Z_L lowers the current. This, of course, lowers the radiated power as well. Column (f) of Table III shows what happens when an energy storage system with at 37Ω load impedance is introduced into the system of Table I column (b). Both the radiated power and the externally required power drop by a factor of 5. This is a consequence of equations (1) and (7). For fixed R_t and R_{ion} we always maintain the same "radiation efficiency" $\epsilon = P_{\text{rad}}/\bar{P}_{\text{ext}}$. This same fact is demonstrated by a comparison of columns (b) and (c) and of columns (d) and (e) of Table III.

Table IV corresponds closely to Table III except that the tether length is taken to be 5 km, which makes both the tether resistance values of columns (a)-(e) and the V_B values smaller by a factor of 4. The degree of improvement in power requirements shown in going from Table III to Table IV depends on the relative values of R_{ion} and R_t . In column (a) we see a decrease by a factor of two in power requirements in going from 20 km to 5 km because $R_{\text{ion}} \sim R_t$ in this column. The improvement is by a factor of 3.7 in column (d).

The external power required for the systems in Table IV range from 0.68 kW to 4.4 kW. This latter value is for 1.25 kW of radiated power at a radiation resistance of 10Ω . In the next six months we will be investigating the kinds of on-board energy storage and collection systems that would be required to operate the type of self-driven tether radiators we have been considering.

We have applied the equations derived from energy considerations in the previous section to obtain the examples presented in Tables I-IV. These results indicate an optimization process that consists of two parts, which are not necessarily independent of each other. The first step is to determine the minimum tether length compatible with wave transmission at the desired frequency and at sufficient power levels. Then, at this minimum length, utilize a tether with the lowest practical resistance value consistent with tether flexibility, mass constraints, etc., in conjunction with an electrical energy storage system and the "self-driven" reversed current mechanism.

Table I

	(a)	(b)	(c)	(d)	(e)
ℓ	20km	20km	20km	20km	20km
R_t	650 Ω	303 Ω	690 Ω	311 Ω	698 Ω
* R_{ion}	50 Ω	10 Ω	10 Ω	2 Ω	2 Ω
i	5A	11.2A	5A	11.2A	5A
V_B	3.5kV	3.5kV	3.5kV	3.5kV	3.5kV
Z_L	0.0 Ω				
$i^2 Z_L$	0.0kW	0.0kW	0.0kW	0.0kW	0.0kW
* P_{rad}	1.25kW	1.25kW	0.25kW	0.25kW	0.05kW
\bar{P}_{ext}	17.5kW	39.1kW	17.5kW	39.1kW	17.5kW

Table I - 20 km tether, no energy storage in natural current phase.

Table II

	(a)	(b)	(c)	(d)	(e)
ℓ	5km	5km	5km	5km	5km
R_t	125 Ω	68.3 Ω	165 Ω	76 Ω	173 Ω
* R_{ion}	50 Ω	10 Ω	10 Ω	2 Ω	2 Ω
i	5A	11.2A	5A	11.2A	5A
V_B	875V	875V	875V	875V	875V
Z_L	0.0 Ω	0.0 Ω	0.0 Ω	0.0 Ω	0.0 Ω
$i^2 Z_L$	0.0kW	0.0kW	0.0kW	0.0kW	0.0kW
* P_{rad}	1.25kW	1.25kW	0.25kW	0.25kW	0.05kW
\bar{P}_{ext}	4.375kW	9.8kW	4.375kW	9.8kW	4.375kW

Table II - 5 km tether, no energy storage in natural current phase.

* R_{ion} and P_{rad} values are unverified assumptions chosen for the sake of comparison.

Table III

	(a)	(b)	(c)	(d)	(e)	(f)	(g)
ℓ	20km						
R_t	100 Ω	303 Ω	650 Ω				
* R_{ion}	50 Ω	10 Ω	10 Ω	2 Ω	2 Ω	10 Ω	50 Ω
i	5A	11.2A	5A	11.2A	5A	5A	2.24A
V_L	3.5kV						
Z_L	550 Ω	203 Ω	590 Ω	211 Ω	598 Ω	387 Ω	865.2 Ω
$i^2 Z_L$	13.75kW	25.4kW	14.75kW	26.4kW	15.0kW	9.675kW	4.3kW
* P_{rad}	1.25kW	1.25kW	0.25kW	0.25kW	0.05kW	0.25kW	0.25kW
\overline{P}_{ext}	3.75kW	13.75kW	2.75kW	12.75kW	2.55kW	7.825kW	3.5kW

Table III - 20 km tether, energy stored in natural current phase, low resistance ($R_{t/\ell} = 5\Omega/\text{km}$) for columns (a) through (e).

Table IV

	(a)	(b)	(c)	(d)	(e)	(f)	(g)
ℓ	5km	5km	5km	5km	5km	5km	5km
R_t	25 Ω	25 Ω	25 Ω	25 Ω	25 Ω	25 Ω	25 Ω
* R_{ion}	50 Ω	10 Ω	10 Ω	2 Ω	2 Ω	10 Ω	50 Ω
i	5A	11.2A	5A	11.2A	5A	5A	2.24A
V_B	875V	875V	875V	875V	875V	875V	875V
Z_L	100 Ω	43.3 Ω	140 Ω	51.3 Ω	148 Ω	96.7 Ω	216.3 Ω
$i^2 Z_L$	2.5kW	5.4kW	3.5kW	6.4kW	3.7kW	2.4kW	1.08kW
* P_{rad}	1.25kW	1.25kW	0.25kW	0.25kW	0.05kW	0.25kW	0.25kW
\overline{P}_{ext}	1.875kW	4.375kW	0.875kW	3.375kW	0.675kW	1.96kW	0.875kW

Table IV - 5 km tether, energy stored in natural current phase, low resistance ($R_{t/\ell} = 5\Omega/\text{km}$) for columns (a) through (e).

* R_{ion} and P_{rad} values are unverified assumptions chosen for the sake of comparison.

4.0 TETHER RADIATION AND THE QUESTION OF TETHER LENGTH

We have seen that, all other things being equal, short tethers require less external power to operate as ULF/ELF radiators. What other factors enter into the determination of the optimal tether length? As a radiator of e.m. waves, the electrodynamic tethered system can be considered from a number of standpoints. It is a well established general principle of antenna transmission theory and practice that an antenna generates e.m. radiation much more efficiently at wavelengths comparable to its own dimensions. For antenna lengths d much shorter than the radiated wavelengths λ , the radiated power falls off as $(d/\lambda)^2$. The wavelength of a 10 Hz wave in free space, or in the atmosphere, is 30,000 km. Thus ELF wave generation from the ground requires very large antennas that have very high input power requirements because of their low radiation resistance. It is this combination of large size and high power that have made such Earth-based ELF antennas environmentally unacceptable.

At 300 km altitude, because of the high plasma index of refraction ($\sim 10^3$) for waves with frequencies much lower than the ion cyclotron frequency (here, around 50 Hz), the wavelength of a 10 Hz wave is only 30 km. The possibility of having an ULF/ELF antenna whose length is of the same order of magnitude as that of the wavelength of the emitted radiation is one of the main reasons orbiting tethers have been considered seriously for the function of transmitting antennas of ULF/ELF radiation. Another factor that encourages consideration of long orbiting tethers as ULF/ELF radiators is that in the ionosphere, waves of this frequency band propagate as Alfvén waves, which travel along the geomagnetic field lines. Thus the radiated power is naturally beamed along the field lines to the atmosphere.

In the preceding paragraphs we have implicitly assumed that the tether acts as a long electric dipole antenna. From this viewpoint there is clearly a strong correlation between the transmitting frequency and the optimal tether length. A half-wave dipole oscillating at 10 Hz in a 300 km orbit would be around 15 km long.

The electric dipole picture of the electrodynamic tether system is far from being a complete description of what is going on, however, because it fails to consider the ionospheric currents. The orbital motion of the tether across the magnetic field lines, along which the ionospheric current flows, means that the tether (an insulated wire with metal electrodes at both ends) is in electrical contact with each field line for only the time it takes the satellite surface (or plasma contactor cloud) to pass by. The tether thus delivers a $vB\ell$ voltage pulse to one pair (at the upper and lower tether ends) of magnetic flux tubes after another. This sends a transmission line type pulse of current (negative at one tether end, positive at the other) travelling with the Alfvén speed down the flux tubes. The current pulses are in the form of Alfvén wave packets. This is the "Alfvén wing" picture (Drell et al., 1965; Williamson and Banks, 1981; Grossi, 1984) of wave transmission. It treats a highly idealized case, and will no doubt have to be modified in the future, but the essential point about the transmission line waves seems likely to stand up.

Thus, even if the current in the tether is periodically reversed, as in the schemes discussed in this report, an analysis of radiation from the tether, viewing only the tether current as the source of classical antenna radiation and not considering the transmission line waves, will be incomplete. The total radiation field would seem to be a combination of: a) dipole radiator type waves that carry no charge; and, b) transmission line type waves associated with the field line currents. It is important to note that the transmission

line pulses always travel away from the tether, no matter what the polarity of the current is.

The transmission line model is illustrated in Figure 4-1. In Figure 4-1(a) the tether current flows upward. At the upper end, positive charge (an electron-depleted region) travels to the right at the Alfvén speed. At the lower end negative charge (electrons) moves to the right at the Alfvén speed. This represents a negative current pulse, as indicated by the arrows that point to the left for the lower Alfvén wing current. We have drawn three separate arrows to indicate the Alfvén wing current at both the upper and lower ends of the tether. This is meant to indicate that the Alfvén wing current lies in more than one plane. We are seeing a projection of it onto the plane of the tether and the field line direction. So, one should think of each arrow, and the field line current it represents, as being in its own separate plane. If the tether is moving in the direction out of the page, then arrows progressively to the right represent current lines in planes progressively deeper into the plane of the page. This is illustrated by the top view shown on the right of the figure. There would be a mirror image Alfvén wing extending to the left, which we have not shown. It is not precisely known how far the Alfvén wings will extend before circuit closure occurs with the neutralization of the positive and negative areas by each other, but it should be on the order of tens of kilometers. Travelling at the Alfvén speed, a pulse will take up to a second to complete the circuit. Thus, if the period of the tether current reversal is smaller than this transmit time, the picture after current reversal looks like that shown in Figure 4-1(b). The Alfvén wing currents of Figure 4-1(a) have now moved farther to the right. New transmission pulses with opposite polarization but still moving in the same direction, have begun to travel down field lines. The tether is still moving out of the page, leaving transmission lines behind as it moves,

so these new (opposite polarity) pulses lie in different planes from those of the original ones. The electric field \vec{E} between the Alfvén wings is indicated. Figure 4-1(c) continues the process into another current reversal and shows the "completion of the circuit" by the combining of the positive and negative current pulses of Figure 4-1(a). The tether's orbital motion and the consequent transmission line waves (Alfvén wings) may limit the applicability of any "phantom loop" analysis of the tether radiator as a magnetic dipole. Only for oscillation frequencies much less than the inverse of the circuit closure time could the tether ionosphere circuit be said to resemble an oscillating loop current. But then the tether will travel so far within an oscillation period (~ 80 km in 10 sec at 300 km altitude) that the analogy again appears shaky.

Whether approached from the dipole antenna aspect or the transmission line aspect, the analysis of tether radiation encounters complicated problems of ionospheric propagation on which much work remains to be done. The ionospheric index of refraction changes significantly over spatial dimensions comparable to the wavelengths under consideration. Not only that, the very character of the radiation even changes when the waves travel into lower regions of the ionosphere, where the ion-neutral collision frequency becomes much greater than the ion cyclotron frequency, thus eliminating the effect of the ions. The Alfvén waves become helicon waves with a whistler-like dispersion relation. The charge-carrying Alfvén wing waves and the dipole radiation waves may not be affected in the same way by these changes along the wave path.

Our tentative view, then, is that the tether radiator is to be considered at the same time a long electric dipole antenna and a generator of ionospheric transmission line waves and that the two wave phenomena are distinct, even though waves are beamed at the Alfvén speed along geomagnetic field lines in both cases.

We have seen that the external power requirement is strongly dependent on the tether length. Simply put, shorter tethers require less external power. We have stated that tether length may be determined by the transmitting frequency and radiated power levels required. The variation of the radiation resistance with tether lengths is quite different for the case of transmission line waves and the case of dipole radiation. As we explain below, the tether length suitable for dipole radiation depends on the altitude of the orbit as well. These differences between the two types of radiation imply different choices of orbital height and tether length and effect the system design in other ways. Thus it is very important to evaluate the two types of waves from the standpoint of propagation to the Earth's surface and information carrying ability. A critical question in regard to the Alfvén wing waves is how strongly they are attenuated by leakage currents across the "wings" before they can deliver their wave energy to the atmosphere.

Keeping in mind that the problem of ionospheric crossing remains to be solved, let us examine the relationship between tether length and the radiation power generated by the tether. Using the bifilar infinite transmission line formula, which should be applicable to the Alfvén wings generated by the tether, we find:

$$R_{line} \approx 120 \left(\frac{v_A}{c} \right) \ln \left(\ell / r_B \right) \Omega \quad (8)$$

where v_A is the Alfvén speed, c the speed of light, ℓ the tether length, and r_B the radius of the flux tube along which current flows. It is immediately apparent that the logarithmic dependence of R_{line} on ℓ allows us to vary ℓ with a relatively small effect on R_{line} . This is in contrast with the results of the original Alfvén wing analysis by Drell et al. (1965), which basically dealt with

a parallel plate transmission line. The appearance of v_A in equation (8) indicates that there is more power into the Alfvén wings at higher altitude, where v_A increases. Table V shows R_{line} for a number of orbital height and tether length combinations assuming r_B is 60 meters independently of the altitude. It should be kept in mind that a higher altitude (above F_2H_{max}) means lower electron density, which could lower the attainable tether current value. Higher altitude also means that there is more ionosphere to be crossed by the waves before they can enter the atmosphere. The advantage of higher altitude for Alfvén wing waves transmission may thus be overstated by the R_{line} values. In fact, if propagation losses increased substantially, the extra power into the transmission line waves would have to be considered a waste.

A half-wave antenna in free space has a radiation resistance of $R_{vac} = 73\Omega$. Following through the derivation of this quantity, but assuming the Alfvén wave index of refraction

$$n_A \simeq c/v_A \quad (9)$$

one obtains $R_{rad} = 73\Omega/n_A$. Booker (1984), in a careful calculation of radiation from a Gaussian dipole meant to be the equivalent of a halfwave linear antenna, obtained $R_{rad} \simeq (50/n_A)\Omega$ for Alfvén wave radiation and $R_{rad} (50/n_A)\Omega$ for slow magnetosonic radiation in the $\omega \ll \omega_{ci}$ range. Thus we assume that making the substitution $R_{rad} \simeq R_{vac}/n_A$ for the radiation resistance in the ionosphere gives the right order of magnitude. The expression for linear antennas much shorter than the wavelength at which they are operating is then

$$R_{rad} \simeq \frac{800}{n_A} \left(\frac{\ell}{\lambda}\right)^2 \Omega \quad (10)$$

for $l \ll \lambda$ with $\lambda = v_A/f$.

At an orbital height of 600 km, the Alfvén speed increases by a factor of around three over its value at 300 km. The index of refraction n_A decreases to around 325. The wavelength of a 10 Hz wave is then around 90 km. A 15 km tether having a radiation resistance of around 0.05Ω at 10 Hz, at 300 km altitude, would have a radiation resistance of around 0.06Ω at 600 km. This situation is to be compared to a factor of 3 increase in the radiation resistance for transmission line waves in going from 300 km to 600 km height while maintaining the same tether length (see Table V). We have not taken into account the orbital motion of the tether in making our estimate of tether antenna type radiation. For the low frequencies we are considering this may not be negligible. Our rough estimates of tether antenna radiation resistances for selected tether lengths and altitudes are given in Table VI.

The Alfvén velocities we have used throughout are daytime values. With reduced ion density, the Alfvén velocities will increase at night. The same comments we have made relative to the change in v_A in going from 300 km orbital height to 600 km orbital height apply to the change in going from day to night. Assuming a factor of 20 decrease in the ion density the radiation resistance for the Alfvén wings will increase by roughly a factor of 4.5 at night. This is shown in Table V. Assuming that this is the dominant form of wave transmission, then it would be possible to reduce the external power requirement by substantial amounts at night while maintaining the same radiated power levels as during the day. The higher the ratio of R_t to R_{ion} , the greater would be the savings in power.

The preliminary results presented in this section and the preceding one indicate that more power is injected into the transmission line "Alfvén wing"

waves than into "tether antenna" waves and that radiated power into the former mode is much less dependent on tether length. If the transmission line waves propagate well through the ionosphere, then these are highly desirable characteristics.

Final conclusions about optimal tether lengths or orbital heights will require a better understanding of propagation of the Alfvén wing waves and the "regular" electromagnetic waves through the ionosphere. We have identified factors that will influence the choice of these crucial system parameters.

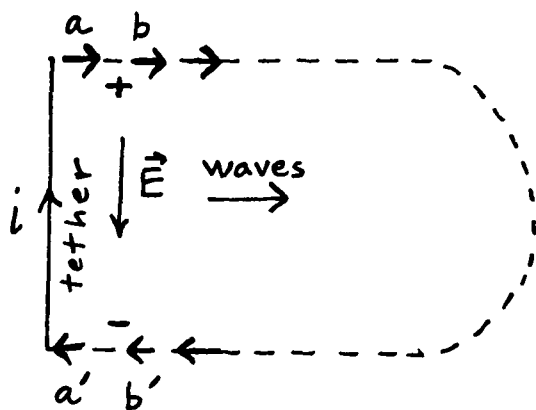


Figure 4.1 (a)

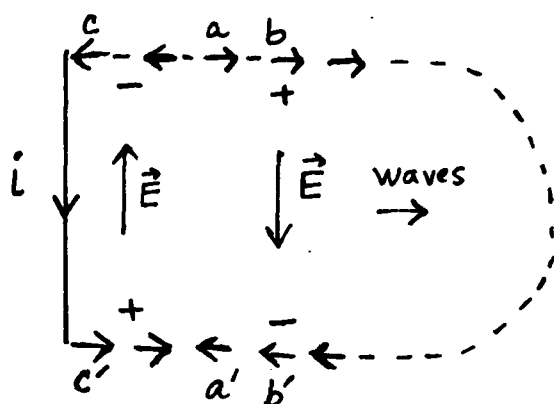
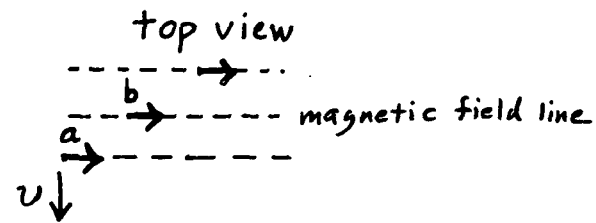


Figure 4.1 (b)

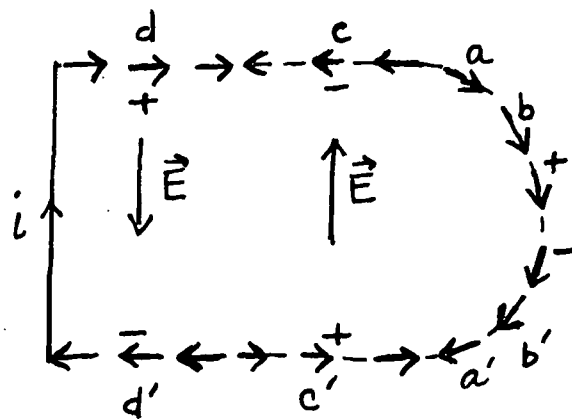
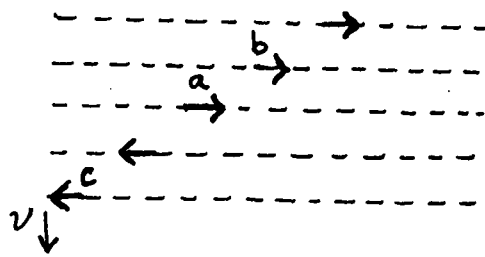


Figure 4.1 (c)

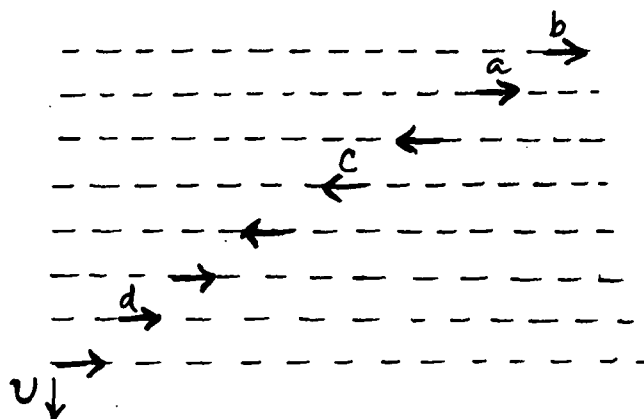


Figure 4.1. The Transmission Line Waves from an Alternating Current Tether System.

Table V

Radiation Resistances for "Transmission Line" Waves

ℓ	5km	5km	10km	10km	2km	2km
h	300km	600km	300km	600km	300km	600km
$R_{\text{rad}}(\text{day})$	0.6 Ω	1.9 Ω	.7 Ω	2.2 Ω	0.5 Ω	1.6 Ω
$R_{\text{rad}}(\text{night})$	2.7 Ω	8.5 Ω	3.1 Ω	9.8 Ω	2.2 Ω	7.2 Ω

Table VI

Radiation Resistance for "Antenna" Waves (10 Hz)

ℓ	15km	15km	30km	30km	50km	100km
h	300km	600km	300km	600km	600km	600km
$R_{\text{rad}}(\text{day})$.05 Ω	.064 Ω	.05 Ω	.16 Ω	.16 Ω	.16 Ω
$R_{\text{rad}}(\text{night})$.045 Ω	.014 Ω	.18 Ω	.056 Ω	.16 Ω	.64 Ω

5.0 SYSTEM CONFIGURATION: ONE TETHER VS. TWO

The analysis carried out in Section 2.0 does not distinguish between the case in which a single tether is deployed and then run alternately in the natural current and reversed current modes and the case in which two identical tethered satellites are deployed as shown in Figure 2.4. The concept of using part of the electrical energy generated in the natural current mode to then supply part of the energy used to power the reversed current mode is the same in either case. We have made a preliminary analysis (Section 6) of the dynamics of the dual tether system and, for the example considered, the mechanical oscillations induced by turning on the current appear to be easily controlled. There are a number of reasons why a single-tether system appears more attractive, however. First of all, there is the obvious one of greater simplicity - only one tether to deploy and control, etc. Then there are the savings in mass when we can subtract the mass of one satellite and tether from the system. This reduction of the system size implies a reduction in cost as well. Furthermore, we cut the aerodynamic drag due to tether and end satellites in half, or perhaps a little more if the lower satellite is the one eliminated. Given the savings in mass and aerodynamic drag, one could have more freedom to increase the tether conductor cross-section, which would lower the tether resistance. As seen in Section 2 this is the single most important method of reducing external energy requirements. Thus, from all these standpoints - simplicity, lower mass, lower drag, lower cost, and possible lower resistance - the single tether system has the advantage. What are the reasons for considering the dual-tether system? First of all, the single tether concept assumes that it is possible to reverse the polarity of the current in a long, orbiting tether at a given desired frequency. It is assumed that hollow cathode plasma contactors are utilized at

each end of the tether. These are "passive" devices that emit a cloud of partially ionized gas which then carries a current from the satellite to the ionospheric plasma. The polarity of this current depends on the sign of the electrical potential difference between the satellite and the ionospheric plasma. The plasma contactor is self adjusting, and new plasma is being emitted continually. In principle, the conductivity of the hollow cathode plasma is so high that the plasma cloud responds very quickly to any change in potential by increasing the electrical current in the appropriate direction. However the plasma cloud is clearly not quite as simple as a length of copper wire in its ability to reverse the direction of current flow in response to an electric field. These devices are being studied both theoretically and experimentally by investigators at SAO as well as a number of other institutions. At present the optimum frequencies for an orbiting antenna system are not known, and the capabilities of hollow cathode plasma contactors for polarization reversal under the required conditions need verification. It seems reasonable to consider the dual tether system since it requires no reversal of ionospheric current at any satellite. The upper and lower satellite currents are either on or off, and the middle satellite maintains the same current direction throughout. Whether or not there is any advantage to having two tethers from the signal strength or information carrying standpoint is another question that we are investigating. At first glance it would seem that at distances much greater than the tether lengths, the radiation from the systems would appear very similar.

6.0 DYNAMICS OF THE DUAL TETHER ULF/ELF SYSTEM

A symmetrical tethered system with three masses, as schematically depicted in Figure 6.1, can be utilized as an antenna for radiating in the ionosphere ULF/ELF waves. The scheme adopted permits pulsing the current alternatively in the upper and lower tether segments in order to produce a square wave with the desired frequency. The upper tether, for example, is generating power during half of the square-wave period while the lower tether is generating thrust during the other half. If external power is supplied to the lower tether, the current flowing in the two tether segments can be made equal. As a result, the thrust will equal the drag and the orbital decay will be reduced to zero. If the pulsing frequency is of the order of a few hertz (or even lower) the system has a quasi-static response since every major oscillation resonant frequency of the system is much lower than that. In-plane and out-of-plane frequencies are of the order of 10^{-4} Hz like the frequency of the lateral oscillation of mass m_2 with respect to the other two masses, taking the design parameters depicted in Figure 6.1. The first harmonic string-like oscillation of each tether is of the order of 10^{-3} Hz due to the low tension and the long tether length. The system will therefore, dynamically, see the train of (for example) positive-going pulses as a continuous function with a steady average value. The same applies to the negative-going pulses.

The dynamics of the ULF/ELF system has been preliminarily simulated according to the considerations reported above. The dynamic model used is a two-dimensional model of the ULF/ELF system with the following assumptions: point masses, circular orbit of the system C.M., straight-line and elastic tethers. The model of the vector B is extremely simplified, having been assumed constant along the orbit.

Results are represented in Figure 6.3a-i while the meaning of the various plotted quantities is depicted in Figure 6.2. Figure 6.3a shows the in-plane angle vs. time. It is evident from the figure that the dynamic response is like the response of a well damped system perturbed from its steady state by a step function. The in-plane damping in our case is provided by a closed loop control algorithm. The system senses the in-plane angle of each tether segment with respect to the local vertical and the automatic controller winds the tether, in or out, proportionally to that signal, with the appropriate phase. Figure 6.3b is the $\theta-\dot{\theta}$ phase plane, and it shows very clearly the efficiency of the damping algorithm. Figure 6.3c depicts the tether length variation of tether #1. It is very similar to the length variation of tether #2 because of the system symmetry. The length variation is due primarily to the in-plane damping control algorithm. Figure 6.3d shows the length variation of the longitudinal damper. The damper is needed for damping out the longitudinal oscillations of the elastic tether. In this simulation the damper is a conventional passive system with spring and dashpot. The damper is tuned to the frequency of the longitudinal oscillation, and its damping coefficient is equal to .9. Figure 6.3e represents the variation of the lateral displacement ϵ of mass m_2 with respect to m_1 and m_3 vs. time. This plot is of little significance because the maximum variation of the quantity ϵ is much smaller than the accuracy adopted in the numerical integration. The plot must be interpreted as a demonstration of the negligibility of the lateral oscillation. The main reason for that being the anti-symmetry of the external perturbation. If the quantity ϵ increases, the same in-plane active damping algorithm discussed above is capable of damping out the lateral oscillation. Figures 6.3f and g show the tension variation in tether #1 and tether #2 respectively. Both figures clearly show that the initial longitudinal tether oscillations due to the imperfect initial conditions and to the onset of the electrodynamic forces are effectively abated by the longitudinal dampers.

Figures 6.3h and i depict the modulus of the electrodynamic force acting upon tether #1 and tether #2 respectively. The actual force is four times greater than what is shown on the plot. A factor of two accounts for the fact that the simulation program is using the average value of each square wave (bear in mind the comments given at the beginning of this section). Another factor of two accounts for the fact that the electrodynamic force in the computer code is applied to the end mass instead of being uniformly distributed along the tether.

The results from this preliminary analysis of the ULF/ELF system dynamics show that the dynamic response is smooth and not critical for a current of 10 Amp. The high frequency of the current modulation makes the external perturbation to be perceived by the system as a continuous step function with the amplitude equal to the average value of the square wave over a period. We think that up to a modulation of a few tenths of a hertz the system dynamic response is independent of the current modulation frequency (at least for the lower harmonics of vibrations). Since the maximum oscillation amplitudes are small for the 10A current (the maximum in-plane angle is around 4°) higher currents could be used. The dynamic response is however dependent on the efficiency of the damping algorithms. Further investigations with the real orbital variation of the B vector and the out-of-plane dynamics are required for a more complete picture of the system dynamics.

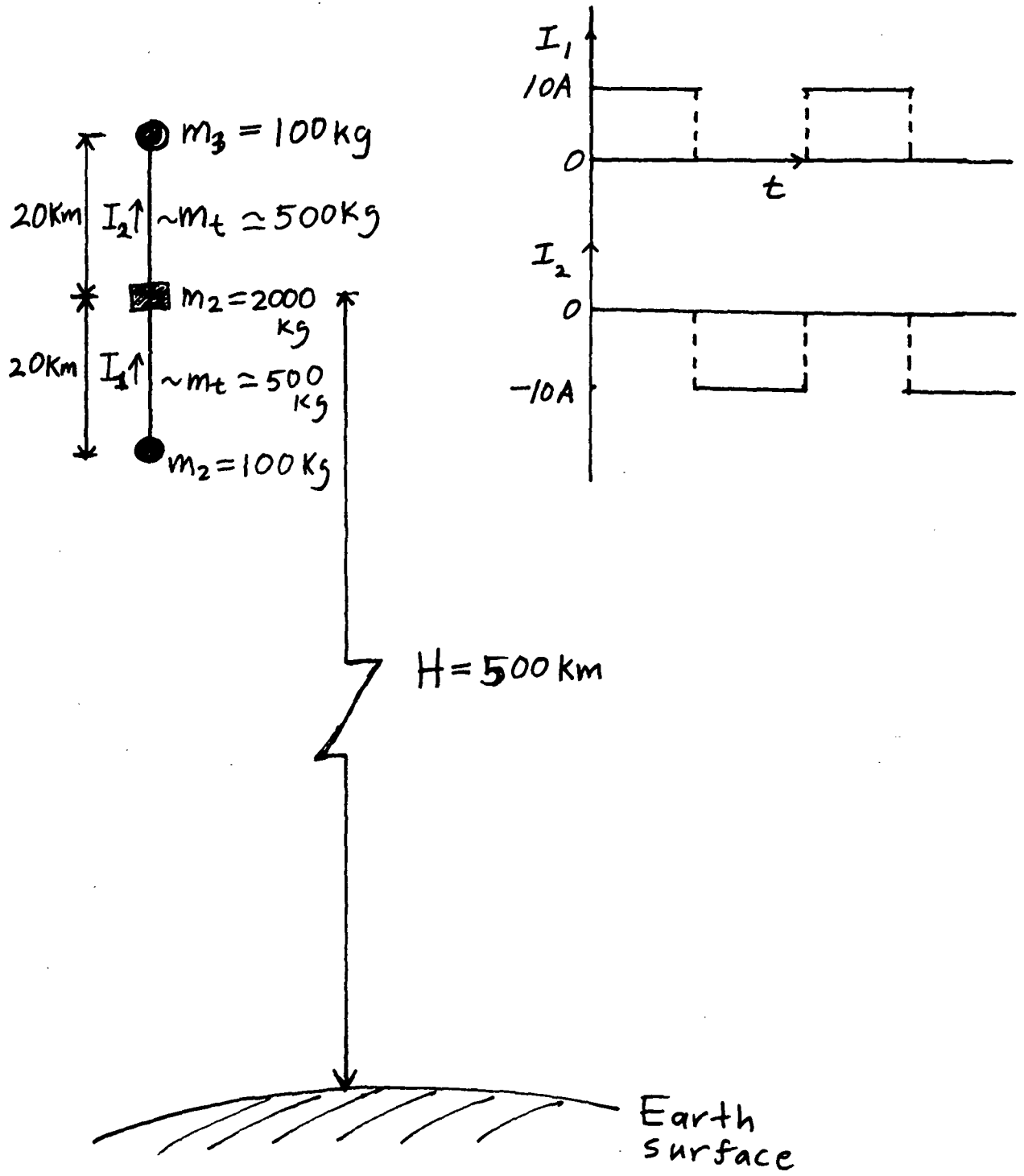


Figure 6.1. The Dual Tether System Simulated in the Dynamics Study

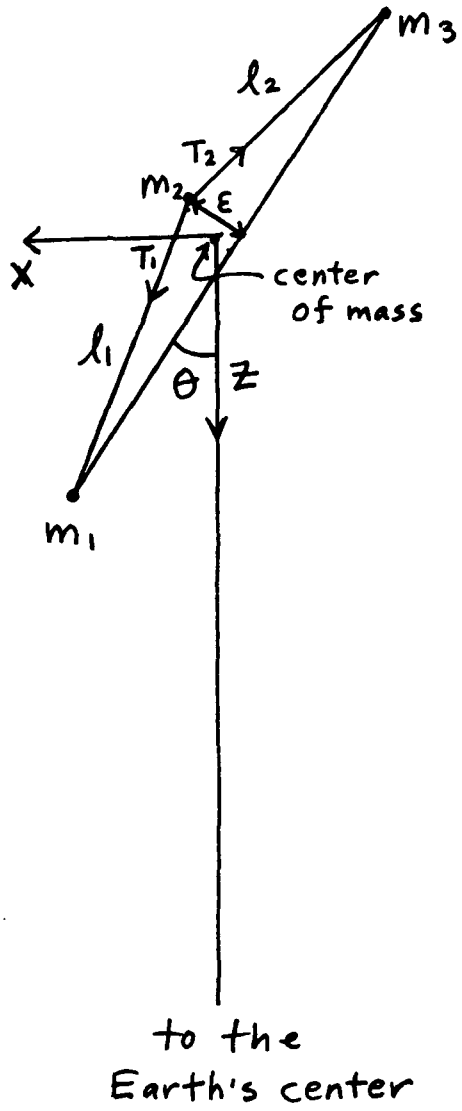


Figure 6.2. Definition of System Parameters for Dynamics Study

Figure Captions

- Figure 6.3a - In-plane Oscillations After Current Startup.
- Figure 6.3b - $\dot{\theta}$ vs. θ After Current Startup.
- Figure 6.3c - l_1 vs. Time After Current Startup.
- Figure 6.3d - Length Variation of the Longitudinal Damper vs. Time After Current Startup.
- Figure 6.3e - m_2 Lateral Deflections vs. Time.
- Figure 6.3f - Tether Tension (T_1) vs. Time.
- Figure 6.3g - Tether Tension (T_2) vs. Time.
- Figure 6.3h - Electrical Force on Tether #1 vs. Time.
- Figure 6.3i - Electrical Force on Tether #2 vs. Time.

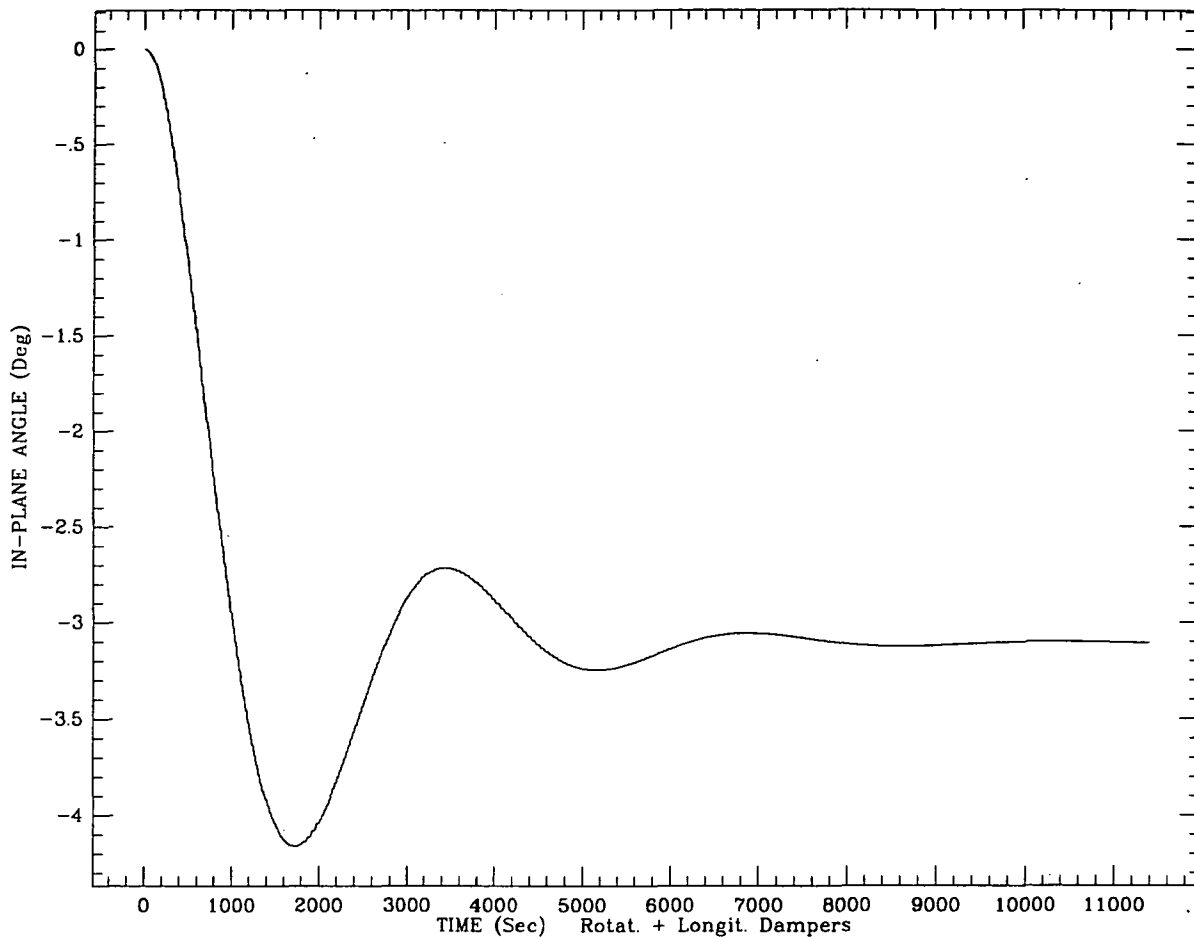
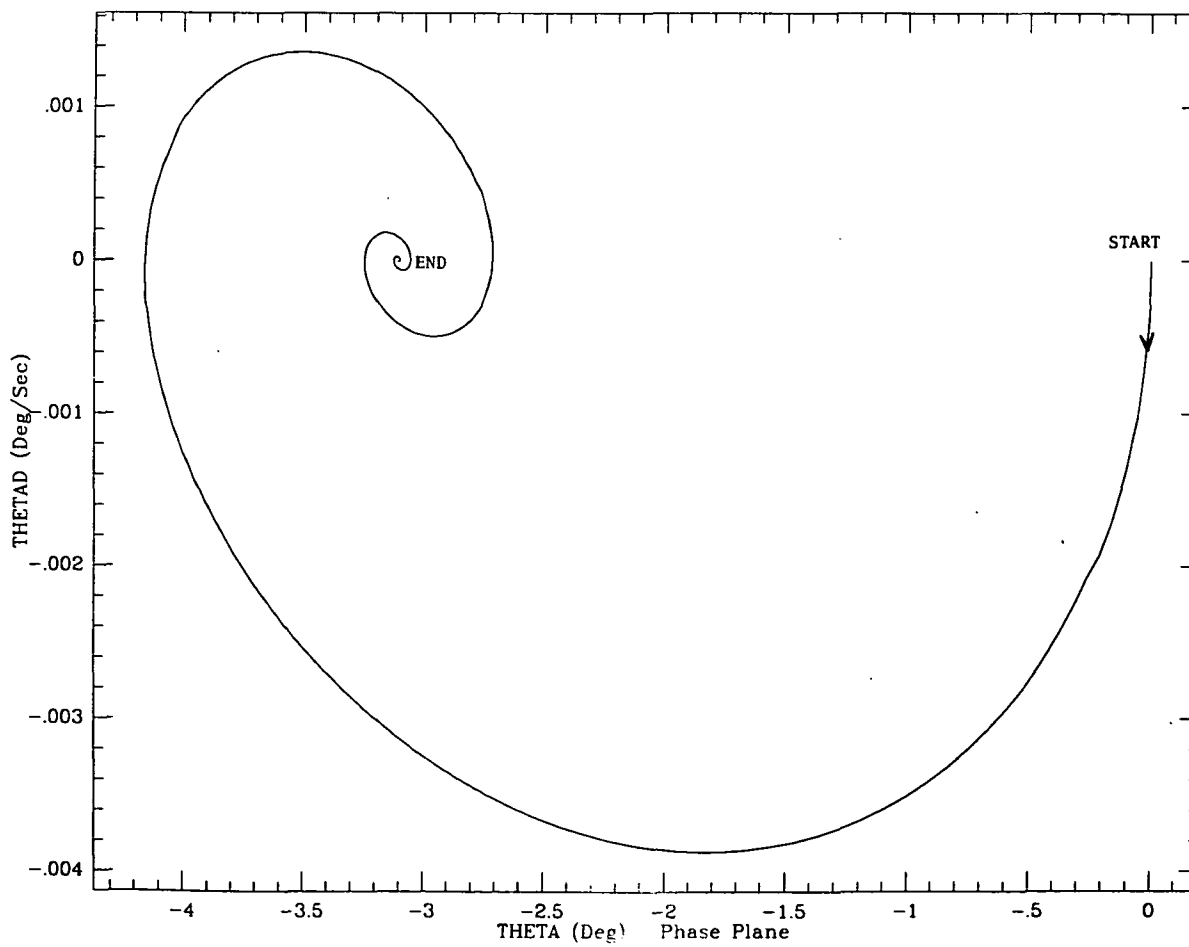


Figure 6.3a†

Figure 6.3b‡



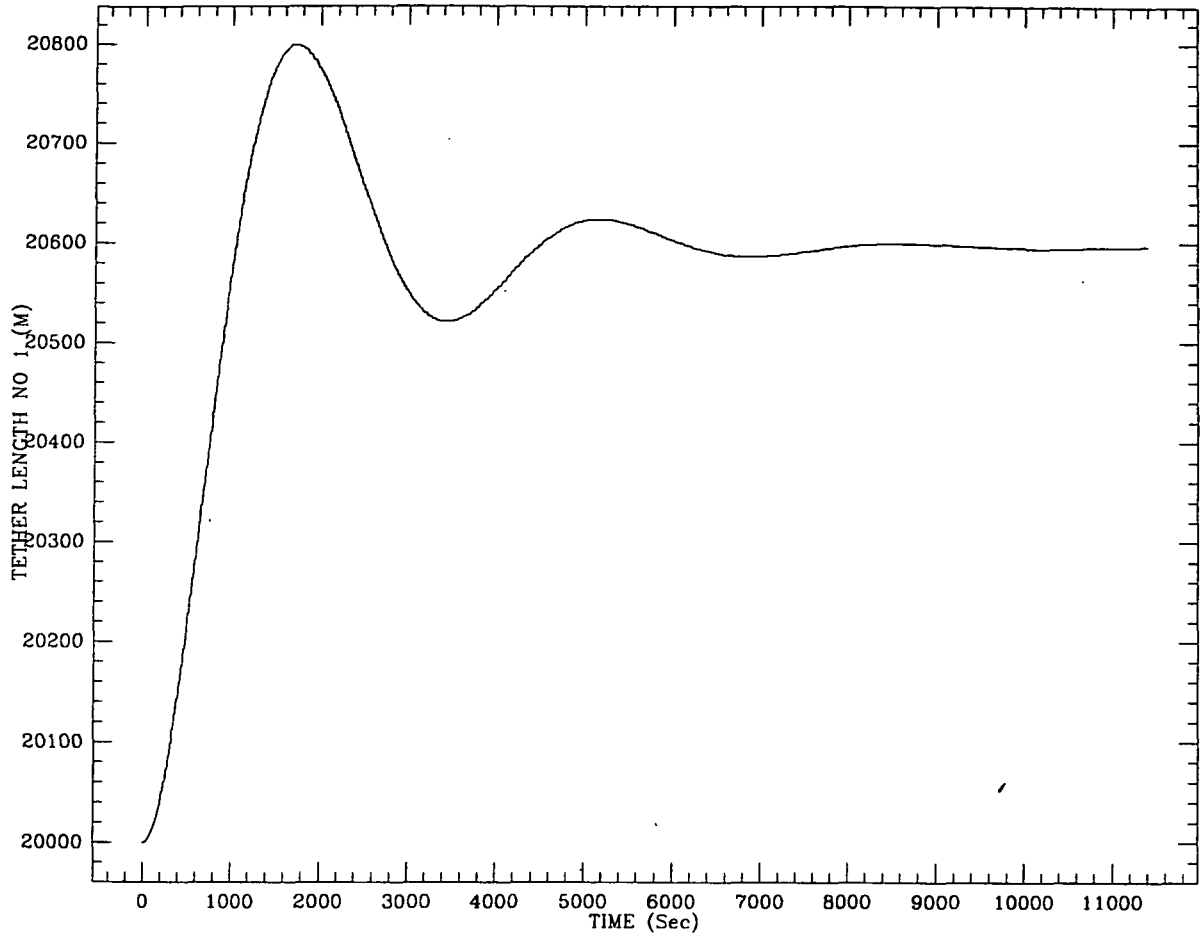
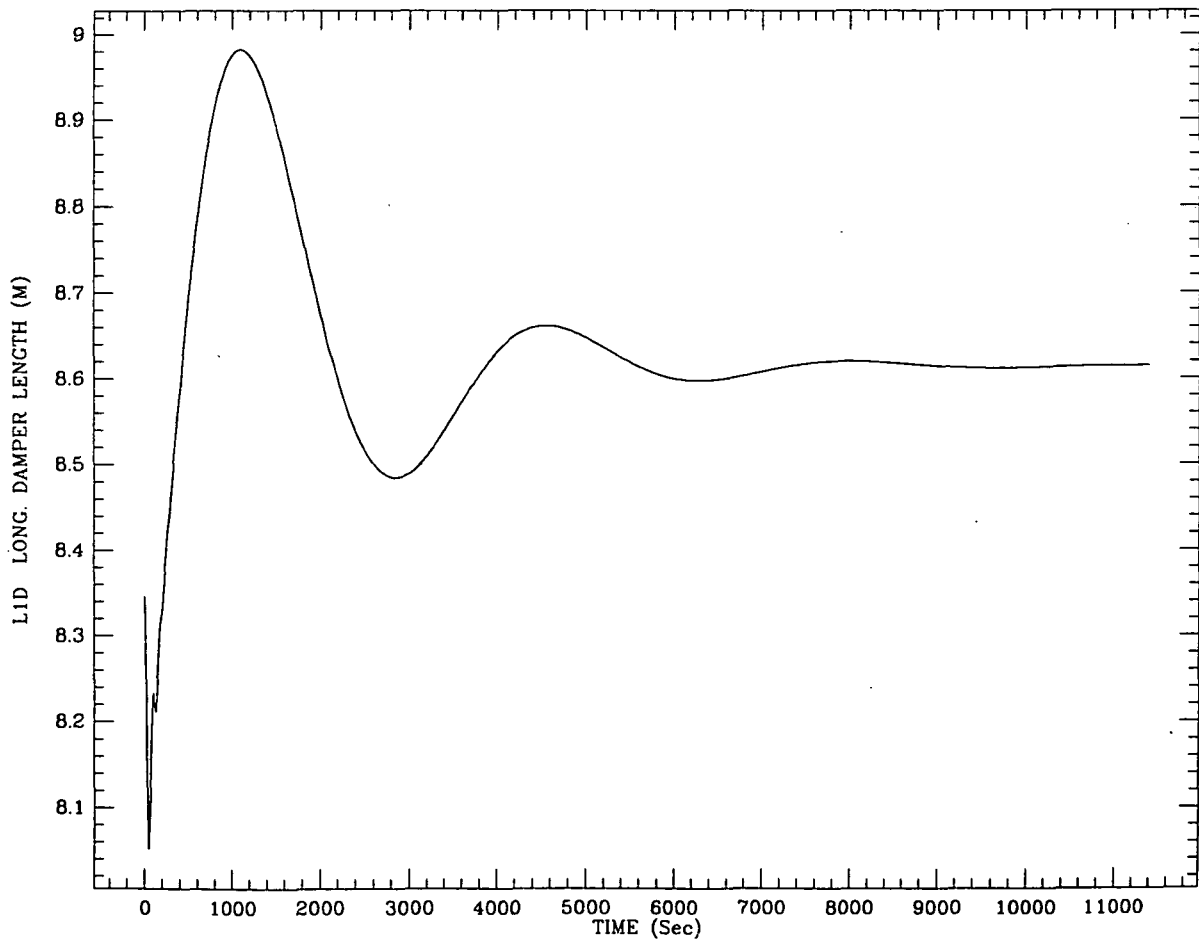


Figure 6.3c†

Figure 6.3d‡



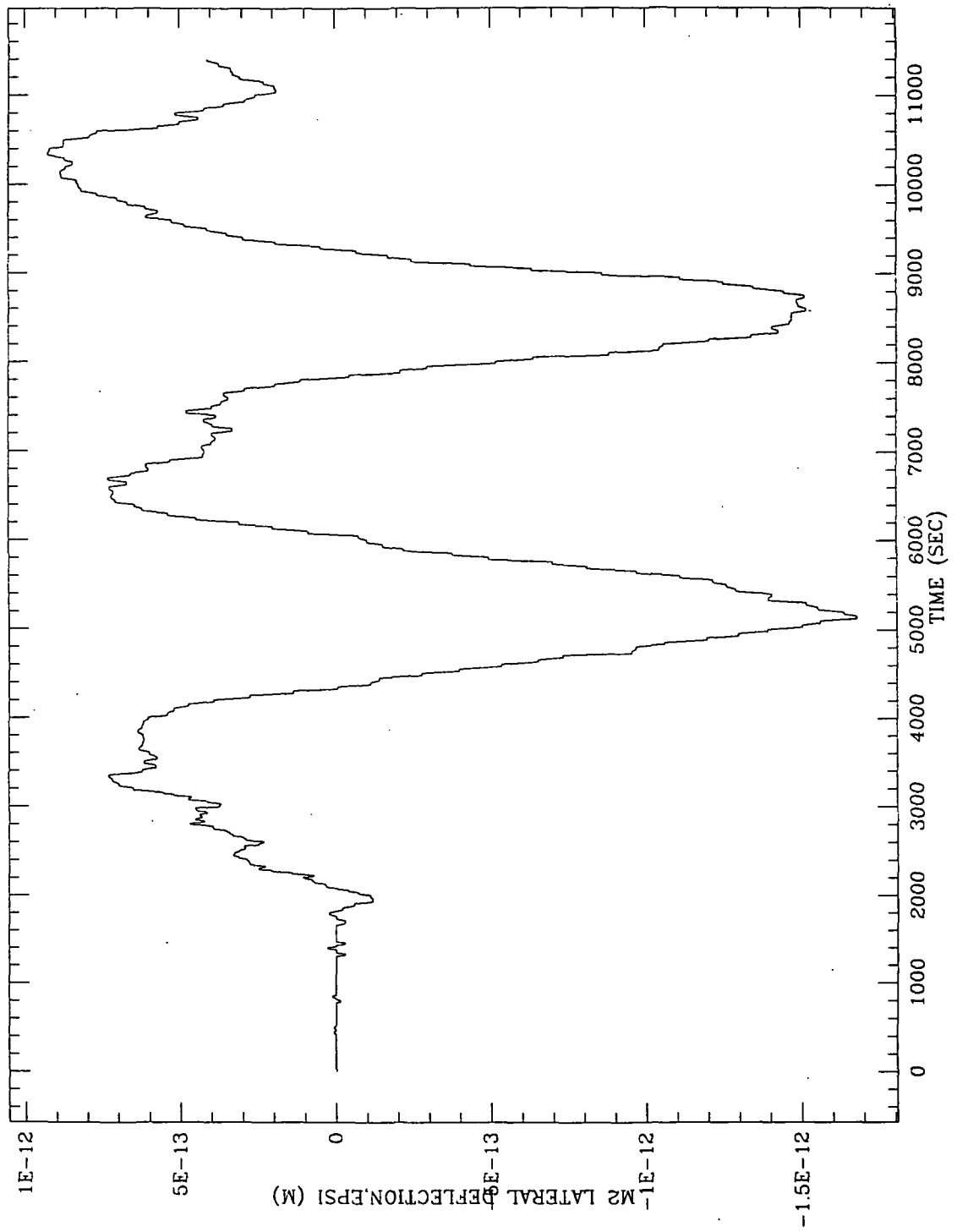


Figure 6.3e

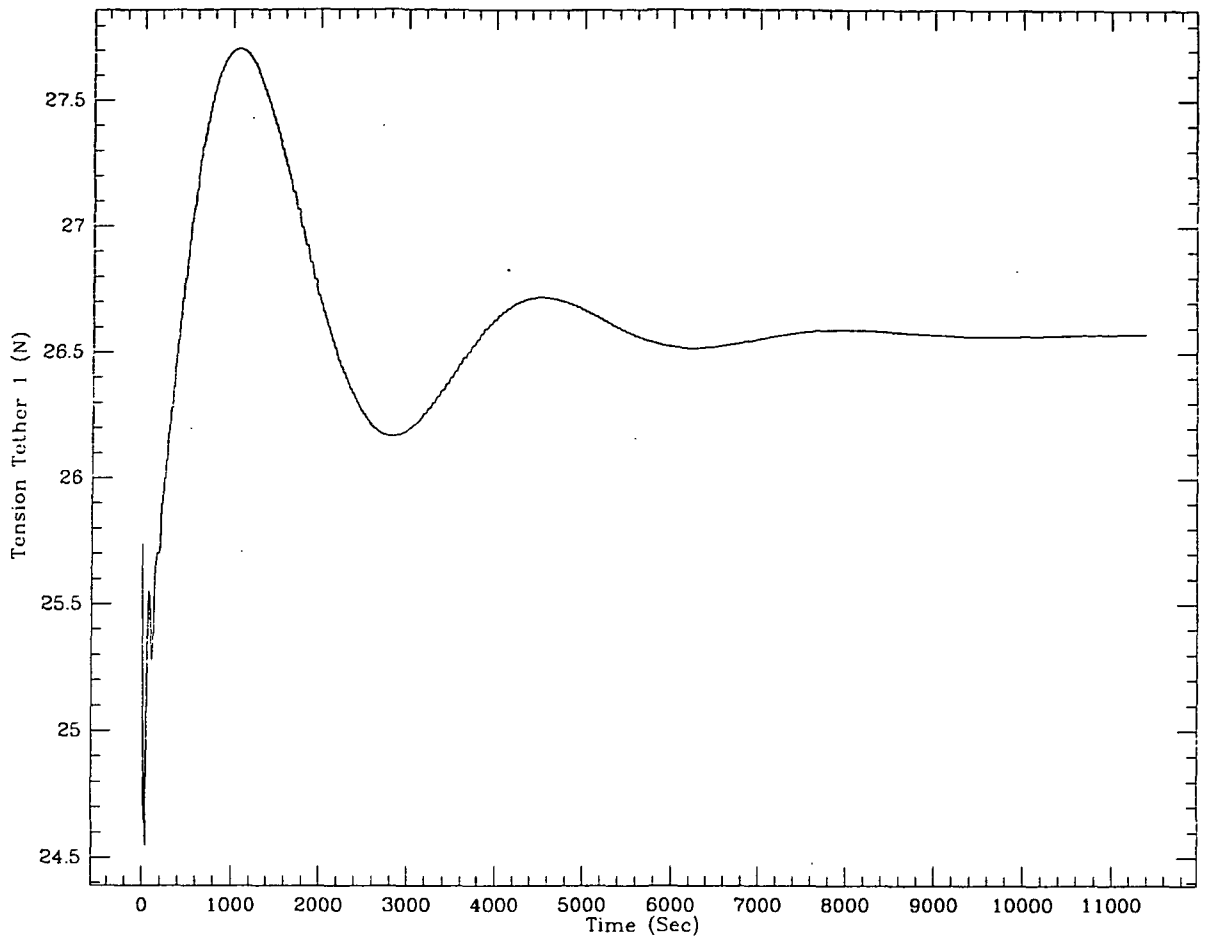
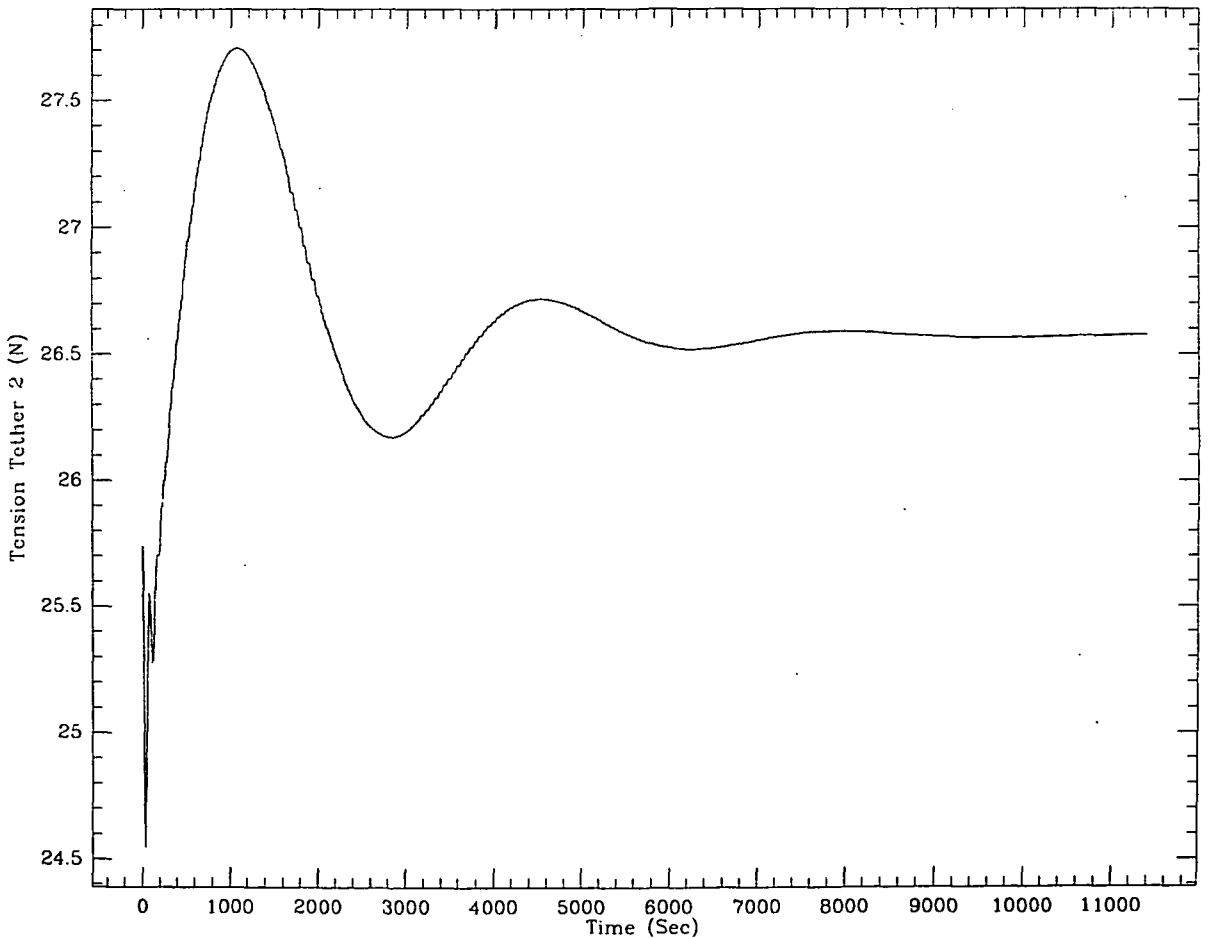


Figure 6.3f†

Figure 6.3g†



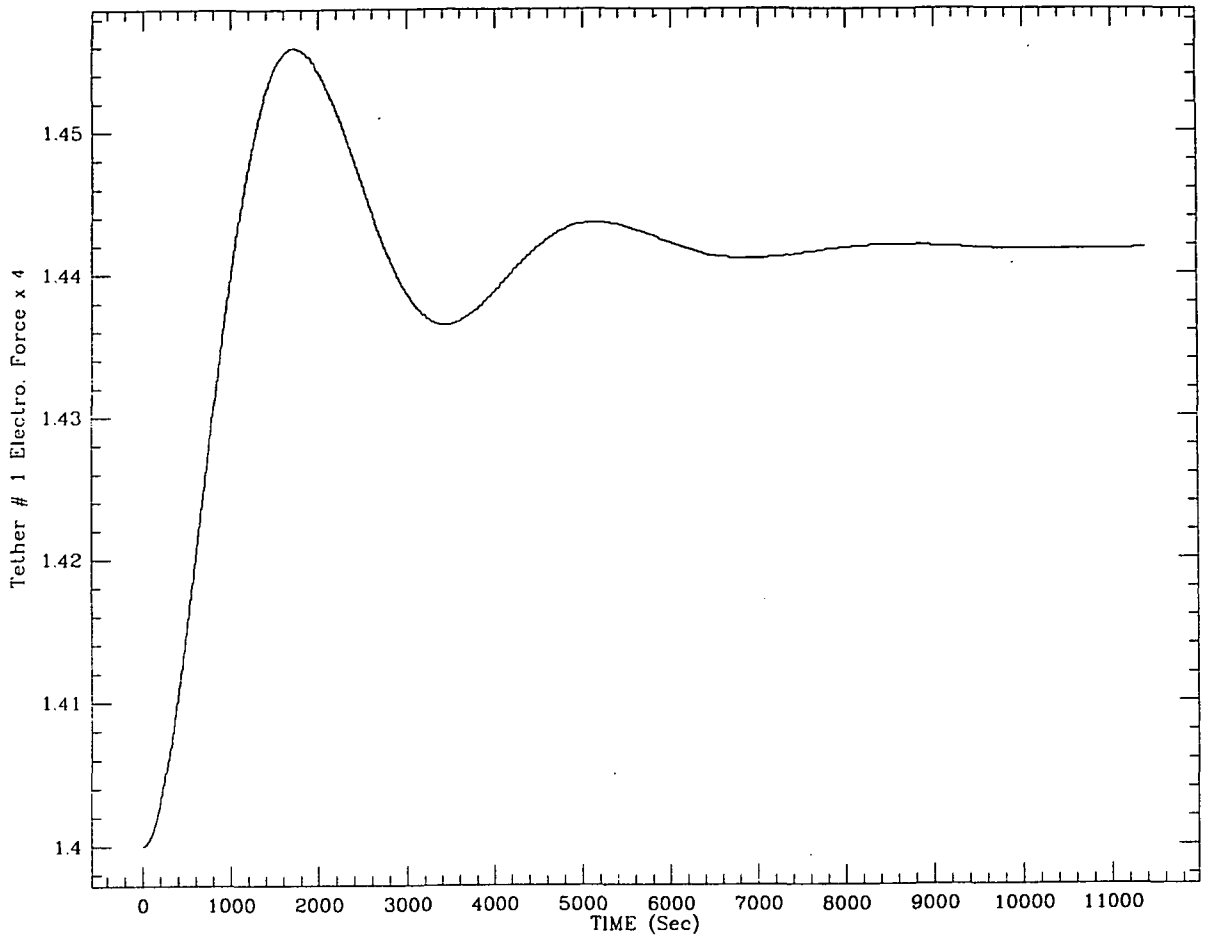
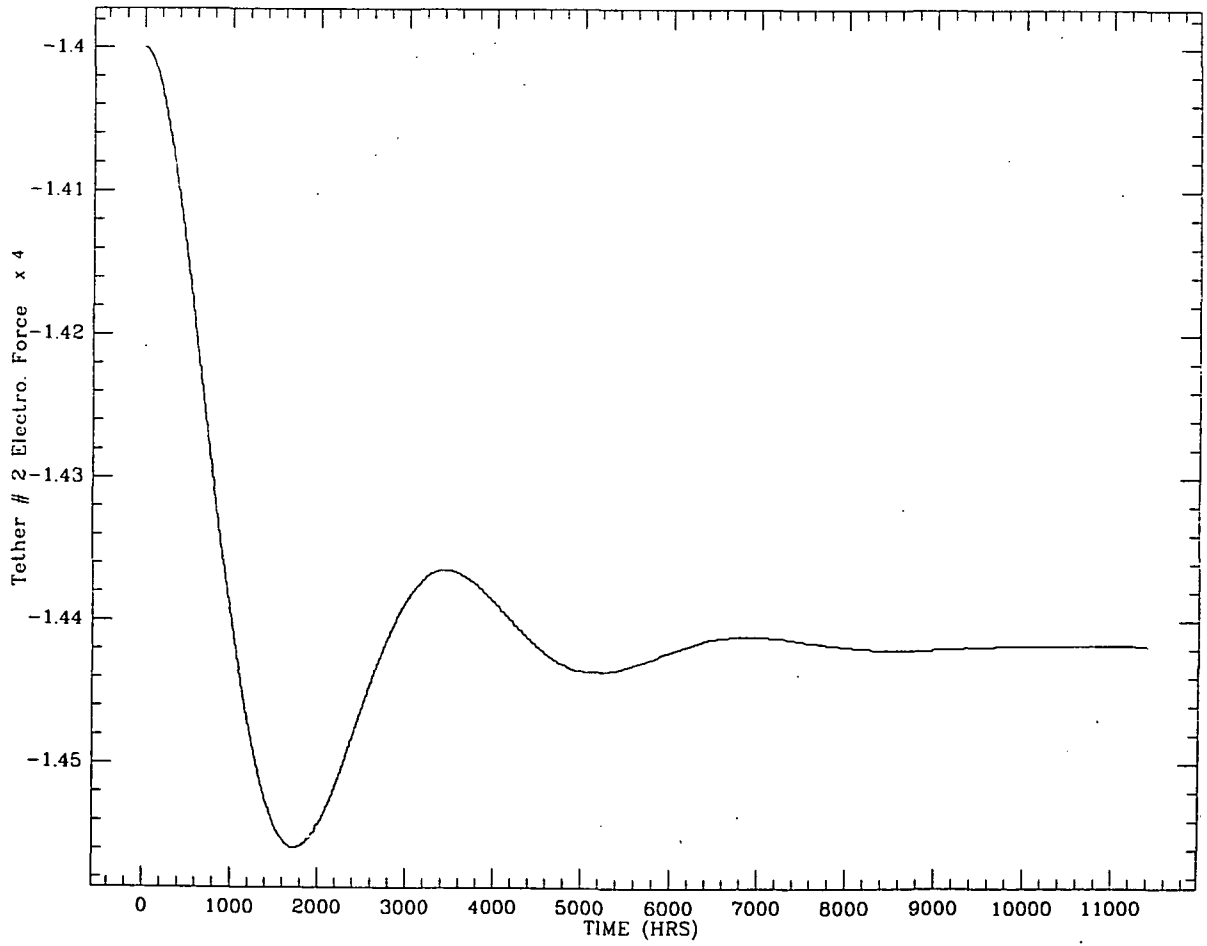


Figure 6.3h†

Figure 6.3i†



7.0 CONCLUSIONS AND FUTURE WORK

The neat concept of combining drag compensation with wave generation through periodically reversing the direction of the current in the tether of an orbiting tethered satellite system has been scrutinized for flaws. We find that the concept is sound. Furthermore, our analysis of the on-board power required to maintain such a system in orbit has shown that long-term, continuous operation of orbiting ULF/ELF transmitters is achievable with moderate power demands through the utilization of this concept, when reasonable assumptions are made about the tether current requirement. Given the complexity of the problem and the absence of relevant experimental data, these "reasonable" assumptions must be considered tentative, however.

The external power requirement can be reduced by shortening the tether (not necessarily an available option), by reducing tether resistance per unit length, and by utilizing the "self-driven" concept, in which part of the electrical energy available in the "natural" current phase of operation is applied to running the system in the reversed current, thrusting phase. The use of this mechanism is only possible when there is "extra" energy available in the natural current phase, i.e. when the motion-induced emf is sufficient to drive a current greater than the one required to reach the minimum allowable signal level. The use of the "self-driven" mechanism necessarily reduces the current level, and in the final analysis that is why it works.

The tether with alternating current generates electromagnetic waves by two separate mechanisms. There are the transmission line waves (Alfven waves) associated with the ionospheric current, and there are the waves generated by the tether in its electric dipole antenna function. The best estimates we can now

make indicate that more power goes into the transmission line waves. A thorough analysis of the wave propagation might show, however, that the "antenna waves" are more important to communications.

A choice between the two types of waves implies differences in system design and operation, since the power radiated depends on tether length and orbital height quite differently in the two cases. Use of the Alfvén wing mode would allow the use of shorter tethers with consequent energy savings.

During the second six months of our investigation we will be giving special attention to the problem of modulation and communications by means of ULF/ELF tether systems. That is, we will be examining means by which information could be transmitted. An idea that appears promising is varying the duration of the natural current phase while maintaining the total period (natural phase plus reversed current phase) constant. In addition, we will concentrate on evaluating different types of power sources and energy storage systems for use in conjunction with ULF/ELF tether transmitters. Thus, at the end of our investigation we expect to have made the concepts much more concrete and practical and to have made clear what the factors that influence system design are.

8.0 REFERENCES

- Arnold, D.A. et al., 1984. Engineering study of the electrodynamic tether as a spaceborne generator of electric power, SAO Technical Report on NASA Contract NAS8-35497, June.
- Barnett, A. and S. Olbert, 1986. Radiation of plasma waves by a conducting body moving through a magnetized plasma, URSI National Radio Science Meeting, Boulder, Colorado, January.
- Booker, H.G., 1984. Guidance and Beaming of Alfvén Waves, Chapter 2.3 in Arnold et al., 1984.
- Drell, S.D. et al., 1965. Drag and propulsion of large satellites in the ionosphere: An Alfvén propulsion engine in space, J. Geophys. Res. vol. 70, pp. 3131-3145.
- Grossi, M.D., 1984. Spaceborne long vertical wire as a self-powered ULE/ELE radiator, IEEE Journal of Ocean Engineering, JOE-9, No. 3, pp. 211-213, July.
- Williamson, R.P. and P.M. Banks, 1976. The tethered balloon current generator: A space shuttle tethered subsatellite for plasma studies and power generation, NOAA Contract USDC/NOAA, 03-5-022-60, Final Report, January.